

Article

Innovative Nafion- and Lignin-Based Cation Exchange Materials Against Standard Resins for the Removal of Heavy Metals During Water Treatment

Sara Bergamasco ¹, Luis Alexander Hein ¹, Laura Silvestri ², Robert Hartmann ³, Giampiero Menegatti ⁴, Alfonso Pozio ² and Antonio Rinaldi ^{1,2,*}

¹ NANOFABER S.r.l., Via Anguillarese 301, 00123 Rome, Italy; sara.bergamasco@nanofaber.com (S.B.); luis.hein@nanofaber.com (L.A.H.)

² TERIN-DEC Division, ENEA—Italian National Agency for New Technologies, Energy and Sustainable Economic Development, Via Anguillarese 301, 00123 Rome, Italy; laura.silvestri@enea.it (L.S.); alfonso.pozio@enea.it (A.P.)

³ Fraunhofer Center for Chemical-Biotechnological Processes, 06237 Leuna, Germany; robert.hartmann@cbp.fraunhofer.de

⁴ MCE Consulting, Piazzale Pizzetti 17, 42012 Campagnola Emilia, Italy; ing.menegatti@mceconsulting.net

* Correspondence: antonio.rinaldi@enea.it

Abstract: The contamination of water by heavy metals poses an escalating risk to human health and the environment, underscoring the critical need for efficient removal methods to secure safe water resources. This study evaluated the performance of four cationic exchange materials (labeled “PS—DVB”, “PA—DVB”, “TFSA”, and “OGL”) in removing or harvesting metals such as copper, silver, lead, cobalt, and nickel from aqueous solutions, several of which are precious and/or classified as Critical Raw Materials (CRMs) due to their economic importance and supply risk. The objective was to screen and benchmark the four ion exchange materials for water treatment applications by investigating their metal sequestration capacities. Experiments were conducted using synthetic solutions with controlled metal concentrations, analyzed through ICP-OES, and supported by kinetic modeling. The adsorption capacities (q_e) obtained experimentally were compared with those predicted by pseudo-first-order and pseudo-second-order models. This methodology enables high precision and reproducibility, validating its applicability for assessing ion exchange performance. The results indicated that PS—DVB and PA—DVB resins proved to be of “wide range”, exhibiting high efficacy for most of the metals tested, including CRM-designated ones, and suggesting their suitability for water purification. Additionally, the second-life Nafion-based “TFSA” material demonstrated commendable performance, highlighting its potential as a viable and technologically advanced alternative in water treatment. Lastly, the lignin-based material, “OGL”, representing the most innovative and sustainability apt option, offered relevant performance only in selected cases. The significant differences in performance among the resins underscore the impact of structural and compositional factors on adsorption efficiency. This study offers valuable insights for investigating and selecting new sustainable materials for treating contaminated water, opening new pathways for targeted and optimized solutions in environmental remediation.

Keywords: ion-exchange resins; sustainable materials; ICP-EOS; adsorption



Citation: Bergamasco, S.; Hein, L.A.; Silvestri, L.; Hartmann, R.; Menegatti, G.; Pozio, A.; Rinaldi, A. Innovative Nafion- and Lignin-Based Cation Exchange Materials Against Standard Resins for the Removal of Heavy Metals During Water Treatment. *Separations* **2024**, *11*, 357. <https://doi.org/10.3390/separations11120357>

Academic Editors: Minhua Su, Changzhong Liao, Dimosthenis Giokas and Jinfeng Tang

Received: 15 November 2024

Revised: 17 December 2024

Accepted: 18 December 2024

Published: 21 December 2024



Copyright: © 2024 by the authors. Licensee MDPI, Basel, Switzerland. This article is an open access article distributed under the terms and conditions of the Creative Commons Attribution (CC BY) license (<https://creativecommons.org/licenses/by/4.0/>).

1. Introduction

The secure and sustainable supply of raw materials has become a fundamental pillar of economic and global development. Metallic elements like copper, lead, cobalt, and nickel are increasingly critical due to their essential roles across numerous sectors, notably in lithium-ion battery production and electric vehicles. Excluding lead, these metals are classified among the 32 raw materials designated as Critical Raw Materials (CRMs) in

Europe, as they are scarce or difficult to source locally and securely [1]. Noteworthy, for example, China dominates global rare earth production [2], while the Democratic Republic of Congo controls around 70% of cobalt supply [3]. This geographical localization of ores/mines and the increasing demand by the industry have the potential to disrupt supply chain and spur significant price volatility, underscoring the need to harvest, reclaim, and reuse these materials [4]. While not presently included on the European CRM list, lead is also a crucial energy material and its recovery is crucial to aid in sustaining the booming battery industry driven by electric mobility and the battery energy storage system (BEES).

On the other hand, the presence of the same metals in industrial wastewater is a real threat and major environmental challenge. Therefore, there is a twofold opportunity to pursue the sequestration of relevant metals to safeguard environment and health, while recovering them for reuse in industry. Significant quantities of precious metals are estimated to be lost to the environment each year through industrial wastewater [5–8]. The sustainable management of this resource requires an integrated approach, one that mitigates water pollution and simultaneously meets the demand to recover valuable materials, thus aligning with sustainable development goals and circular economy principles.

Technological advances in heavy metal recovery from aqueous solutions have evolved considerably in recent years, striving for greater efficiency and sustainability, while minimizing environmental impact.

Among the various methodologies developed to counteract heavy metal pollution, flotation is widely employed. This technique relies on the generation of air bubbles to separate metals from the aqueous matrix [9]. Over time, several variants of this process have been developed, including dissolved air flotation, ionic flotation, and precipitation flotation. In the case of dissolved air flotation, the operating principle is based on the creation of bubbles. The success of this technique depends on various factors, such as the bubble generation method, their size, and the characteristics of the particles to be removed. The ionic variant uses surfactants to bind to metal ions, forming hydrophobic complexes that adhere to air bubbles and are removed as surface foam. This approach offers advantages in terms of energy consumption, ease of management, and operational costs by using surfactants with charges opposite to the target metals. Regarding precipitation flotation, it utilizes specific precipitating agents that combine with the target ions, causing their precipitation [10].

White flotation has proven effective in specific scenarios; other techniques such as ion exchange resin (IER) technology have garnered particular attention for their effectiveness in heavy metal sequestration in water treatment applications [11,12]. Ion exchange processes allow for the selective removal of ions from the aqueous medium, and specific resins enable selectivity based on ion charge and size. These methods have proven especially effective for removing metals such as lead, copper, nickel, silver, and others [13–17].

Conventional resins are often based on polymer matrices functionalized with sulfonic and/or carboxylic groups for cation exchange and amine groups for anion exchange. Their removal efficiency can vary significantly depending on operating conditions, such as pH value, temperature, and metal competition in the treated water [18]. Selectivity for specific metals is often suboptimal, requiring multiple treatment cycles to achieve the desired purification standards. These limitations have spurred research into alternative approaches, focusing on innovative materials that can deliver superior performance while maintaining economic and environmental sustainability.

Cation exchange resins modified with sulfonic groups show remarkable adsorption capacity and selectivity toward various cations present in aqueous solutions, making them valuable tools in water treatment [19]. The cation exchange process with resins functionalized with carboxylic groups plays a crucial role in determining ion exchange properties. The presence of these groups allows for widespread use in water treatment applications. Carboxylic-group-loaded cation exchange resins have proven effective in capturing metals such as copper (Cu), iron (Fe), and manganese (Mn) under controlled pH conditions [20].

In this context, exploring and benchmarking alternative ion exchange materials is essential. This study covered four material options. The first material was Nafion, the brand name for a popular ionomer consisting of sulfonated tetrafluoroethylene-based fluoropolymer–copolymer. While not an obvious choice from a sustainability standpoint, the novelty lies in its second life reuse: the Nafion included in this study was recovered and recycled at ENEA and Nanofaber through physical methods [21], demonstrating an innovative approach to valorize the sophisticated and expensive material within a circular economy framework. This represents a significant advancement in the sustainable use of advanced polymers for engineering applications. The high cation exchange capacity and ionic conductivity make Nafion ideal for water purification applications [22,23]. Nafion's chemical structure, featuring highly hydrated sulfonic groups, facilitates rapid interactions with metal cations in wastewater. This polymer can form cationic complexes, enabling the adsorption of heavy metals such as Ni(II), Co(II), Pb(II), Cu(II), and Ag(I) [24].

The second candidate included in this study was lignin, a natural and highly sustainable biopolymer. It is not only an abundant industrial by-product, but also offers unique chemical properties that can be tailored for enhanced performance. Its use as a metal getter represents a novel and ambitious choice for the application at hand, aligning strongly with the principles of circular economy. Lignin's abundant availability and its intrinsic environmental sustainability make it an impactful biomaterial in the transition toward greener technologies. Lignin's chemical structure, rich in functional groups such as phenolic, hydroxyl, and carbonyl groups, promotes various interactions—ion exchange, complexation, and electrostatic interactions—that are essential for heavy metal adsorption [25,26]. In particular, lignin fractionated via the Organosolv process possesses a heterogeneous surface chemistry with a high density of functional groups that can attract highly charged metal ions [27]. The ion exchange process in lignin involves the substitution of mobile hydrogen ions from the carboxylic and phenolic groups with metal cations [28], enabling effective heavy metal removal from wastewater. A critical advantage of lignin is its versatility, as it can undergo chemical modifications, such as grafting functional groups or forming composites with other materials, to significantly enhance its adsorption capacity and selectivity for specific metal ions [29]. These transformations not only improve lignin's performance, but also expand its applicability, positioning it as a highly adaptable and promising alternative to conventional, less sustainable ion exchange resins. Moreover, its biocompatibility and environmental friendliness further reinforce its appeal as a green material for advanced water treatment technologies.

The first and second cation exchange materials in this preliminary study are reference systems represented by commercially available engineered resins.

In this work, we present an innovative comparative analysis of the performance of four cation exchange materials: two commercially available resins based on poly-styrene-divinylbenzene (PS—DVB) and polyacrylic-divinylbenzene (PA—DVB), and two materials not conventionally used for this application, consisting of a sulfonated tetra-fluoroethylene-based material (TFSA) derived from recovered Nafion and Organosolv lignin (OGL), recognized as a sustainable and naturally sourced material. The analysis focuses on metal removal efficiency, selectivity, and adsorption kinetic parameters, providing a detailed overview of the potential and limitations of these materials for the purification of water contaminated with heavy metals of interest, such as Cu^{2+} , Pb^{2+} , Co^{2+} , and Ni^{2+} (additional results on Ag^+ are reported in the Supplementary Materials). The ion exchange capacities of the different metal–resin pairs were evaluated through batch experiments, quantifying the metal sequestration via ICP-OES analysis and correlating the results with an analysis of the kinetic parameters. This experimental study serves as a fundamental starting point for understanding the actual potential of the tested materials. The findings suggest ample opportunities for optimization, paving the way for their application in both industrial and environmental contexts, with a particular focus on the recovery of critical resources in alignment with circular economy principles.

2. Materials and Methods

2.1. Materials

Sodium chloride, nickel (II) sulphate hexahydrate, cobalt (II) sulphate heptahydrate, lead (II) nitrate, and copper (II) sulphate pentahydrate were provided by Sigma Aldrich, and silver sulphate was provided by BDH Chemicals Limited (Poole, England). The Multielement standard solution I for ICP was provided by Merck (Merck Life Science S.r.l., Milan, Italy). The commercial resins Resinex™ KW-8 and Resinex™ KW-H Na were provided by Poirino srl (Buttigliera d'Asti, Italy) in partnership with Nanofaber (Nanofaber S.r.l. Rome, Italy), Nafion was recovered using a technology developed by Enea (ENEA, Rome, Italy) in partnership with Nanofaber, and the Organosolv lignin was produced in-house at Fraunhofer CBP (Leuna, Germany). A representative photograph of the resins is shown in Figure 1.

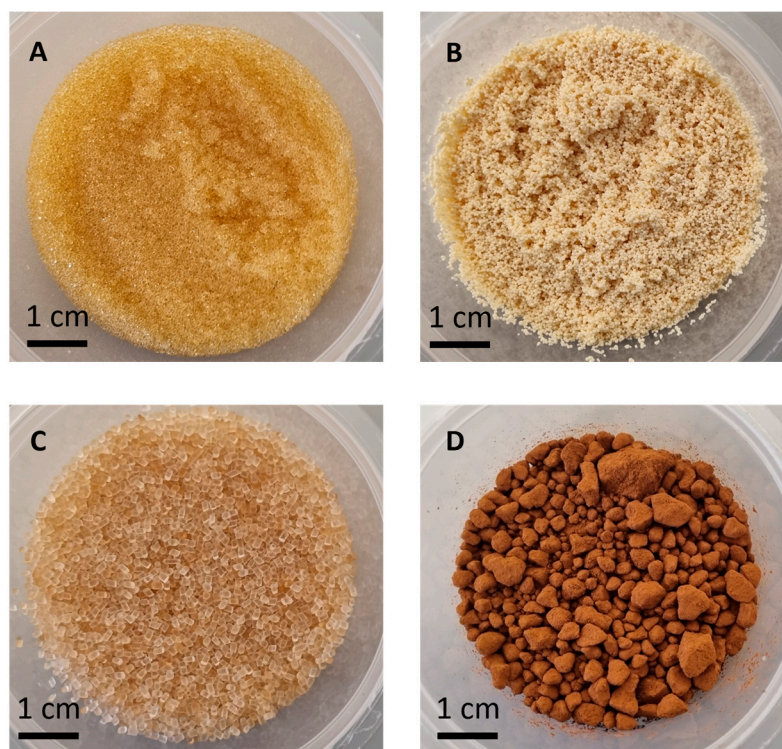


Figure 1. Photographic images of the ion exchange materials utilized: (A) polystyrene-divinylbenzene resin (PS-DVB), (B) polyacrylic-divinylbenzene resin (PA-DVB), (C) regenerated Nafion granules (TFSA), and (D) lignin-based powder material (OGL).

2.2. Methods

2.2.1. Preparation of Synthetic Solutions with a Known Concentration

For each ion exchange material, five monometallic solutions with specific ionic concentrations were prepared, using Milli-Q water to ensure purity. Specific concentrations were prepared for each metal salt to obtain single-metal solutions with known concentrations, specifically 600 ppm of Cu^{2+} , 4000 ppm of Pb^{2+} , 2100 ppm of Co^{2+} , 1200 ppm of Ni^{2+} , and 2000 ppm of Ag^{+} .

2.2.2. Adsorption Test and Instrumental Analysis Using ICP-EOS

For the adsorption tests, 20 batch experiments were conducted, pairing each synthetic monometallic solution with each ion-exchange resin. In each experiment, 0.4 g of resin was used, placed in contact with 20 mL of a solution at a known concentration. The PS-DVB and PA-DVB resins did not require any pretreatment, as they were already loaded with Na^{+} ions, while the TFSA and OGL resins were pretreated overnight in a 15% (w/v)

NaCl solution. To assess metal adsorption by the materials/resins, solution aliquots were taken at intervals of 5, 10, 20, and 40 min. The aliquots were diluted and filtered using syringe filters with a pore size of 0.22 μm , and the resulting samples were analyzed by inductively coupled plasma optical emission spectroscopy (ICP-OES Agilent 5800 ICP-EOS, Santa Clara, CA, USA). Calibration curves were previously prepared for each metal, starting from a multi-element standard solution assessing adsorption based on specific wavelengths (λ).

2.2.3. Evaluation of Cation Exchange and Adsorption Kinetics

The data obtained by analyzing sample aliquots at defined time intervals provided, for each metal–resin pair, the quantity of the metal ions remaining in solution. From these data, the percentage of removal after 40 min can be determined using the following Formula (1):

$$\text{Removal (\%)} = \frac{(C_i - C_f)}{C_i} \times 100 \quad (1)$$

where C_i represents the initial concentration of metal ions in the bulk of the solution at time zero, and C_f is concentration of metal ions in the bulk at equilibrium.

These results enabled a study on the adsorption kinetics and ion exchange capacity. Generally, the adsorption data obtained for most metal-resin combinations can be adequately described through empirical mathematical models. Numerous investigations have attempted to elucidate the correlation between experimental data and pseudo-first-order (PFO) or pseudo-second-order (PSO) models, focusing on the specific type and dynamics of the adsorption processes involved. Some experimental observations, reported in the literature, indicate that at high initial solute concentrations, the adsorption process predominantly follows first-order kinetics. Conversely, at lower initial concentrations, the experimental data exhibit superior conformity to the pseudo-second-order model [30].

An alternative interpretation of model preference is predicated on the chemical characteristics of the phenomenon. Specifically, adsorption processes that conform to the PFO model are typically associated with physical adsorption (physisorption), primarily governed by the availability of vacant sites on the material/resin surface. Conversely, processes following the PSO model are attributed to chemical adsorption (chemisorption) [31], characterized by specific chemical interactions between the metal ions and the functional groups present on the material/resin matrix.

In this work, Lagergren's pseudo-first-order (PFO) (Formula (2)) and pseudo-second-order (PSO) equations (Formula (3)) were applied to model the kinetic data:

$$\log(qt - qe) = \log qe - K_1 t / 2.303 \quad (2)$$

$$\frac{t}{qt} = \frac{1}{K_2 \times qe^2} + \frac{t}{qe} \quad (3)$$

These equations allow for the determination of the equilibrium adsorption capacity qe_{calc} . (in mg of metal per g of material/resin), which can then be compared with the experimentally (qe_{exp}) obtained value to estimate the error on qe (Error qe).

3. Results and Discussions

The results obtained for each material under consideration focus on their ion exchange capacities, metal removal efficiencies, selectivity, and adsorption kinetics. These aspects are evaluated to understand the performance and suitability of each material system for specific metal ions, providing insights into their potential applications and limitations. For convenience and readability purposes, all four materials will be referred to as “resins” in the remainder of the discussion, although only the two commercial materials are actual resins. The following paragraphs detail the observed adsorption behaviors, highlighting differences in resin efficiency and kinetic properties across various combinations of metal–resin pairs.

3.1. Metal Removal Efficiency and Resin Selectivity

Figure 2 shows the removal trends of four metal ions (Cu^{2+} , Pb^{2+} , Co^{2+} , and Ni^{2+}) using the four different cation exchange resins over a contact period of 40 min, with the results for Ag^+ available in the Supplementary Materials. Looking at the Cu^{2+} in Figure 2, we can observe an initial Cu^{2+} concentration of approximately 600 ppm across all resins. PS—DVB proved to be the most effective resin, reaching concentrations of approximately 200 ppm in the first 5 min and achieving near-complete removal (<50 ppm) within 40 min. PA—DVB showed moderate efficiency, reducing the concentration to 230 ppm by the end of the treatment. TFSA exhibited similar but slightly better performance compared to PA—DVB, reaching approximately 400 ppm. OGL demonstrated the poorest performance, maintaining consistently high concentrations throughout the treatment period.

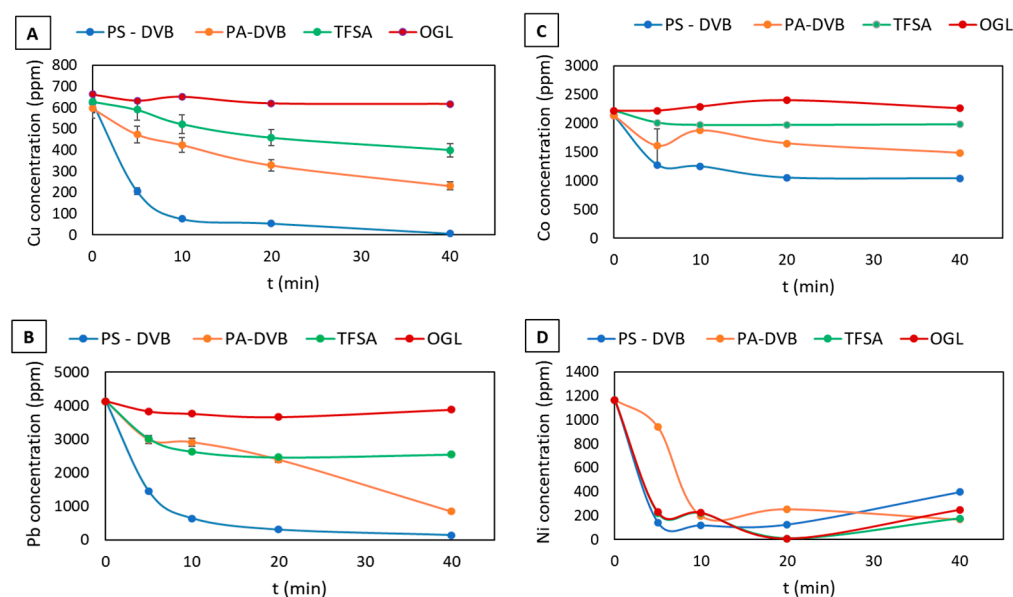


Figure 2. Time-dependent concentration of the available metal ions (Cu^{2+} , Pb^{2+} , Co^{2+} and Ni^{2+}) in bulk solution (ppm) examined by ICP-EOS. Each panel shows the remaining concentration of a specific metal ion over time (0, 5, 10, 20, and 40 min): (A) Cu^{2+} concentration in bulk, (B) Pb^{2+} concentration in bulk, (C) Co^{2+} concentration in bulk, and (D) Ni^{2+} concentration in bulk.

In relation to Pb^{2+} , we started with an initial solution concentration at 4000 ppm. PS—DVB demonstrated effective removal, reaching a concentration of 150 ppm in 40 min. The removal achieved by PA—DVB was good but more gradual, reaching 850 ppm. TFSA plateaued after 5 min around 2500 ppm, while OGL showed minimal removal capacity, maintaining concentrations close to the initial levels. In the case of Co^{2+} , the individual performance was quite limited, except for the PS—DVB resin, which showed good adsorption within 5 min and remained constant up to 40 min. The removal pattern for Ni^{2+} showed more interesting features. Starting from solutions at concentrations of 1200 ppm, all resins showed a rapid initial removal within the first 10 min. PS—DVB and TFSA reached similar final concentrations of 170 and 176 ppm, respectively, while PA—DVB showed some concentration fluctuations before stabilization.

Nafion has proven to be an excellent material for water treatment due to its unique chemical structure, characterized by the presence of polar groups such as sulfonic acids. These functional groups not only enable specific interactions with metal cations, but also provide the material with exceptional water and ion management capabilities. The study conducted by Mashio et al. [32] offers valuable insights into the crucial role of sulfonic groups in ionic interactions. These functional groups are pivotal for cation exchange activity, as they attract metal cations through strong electrostatic interactions. The research highlights how Nafion promotes the formation of hydrophilic clusters that facilitate ion

transport. Although the study primarily focuses on proton transport, it can be inferred that metal cations, due to their positive charge, are effectively captured by the material’s sulfonic groups. Nafion’s ability to modulate its degree of hydration and the internal distribution of water is an additional factor that enhances both the mobility and adsorption of metals.

Unlike Nafion, OGL has a completely different chemical structure, which results in significantly distinct behavior. Lignin is a heterogeneous and branched polymer, rich in hydrophobic aromatic units and functional groups such as methoxyl and hydroxyl groups, which limit its compatibility with aqueous environments. This inherent hydrophobicity can hinder its interaction with water, a crucial factor in systems relying on efficient cation exchange. Consequently, lignin’s reduced hydration capacity may compromise the formation of hydrophilic domains necessary for ion mobility and adsorption. Although lignin contains some polar functional groups, such as phenolic hydroxyls and carboxylic acids, their lower density and accessibility compared to the sulfonic groups of Nafion further reduce its efficiency in the exchange of metal cations in solution. These characteristics highlight the challenges associated with using lignin in applications requiring strong water affinity, making its chemical engineering essential to transform it into a competitive material.

3.2. Kinetic Models for the Absorption of Heavy Metals

The kinetic analysis of the adsorption processes for different metal–resin systems allowed for the identification of characteristic models underlying the interactions between metal cations and the functional groups of the resins investigated (Table 1). The use of pseudo-first-order (PFO) and pseudo-second-order (PSO) kinetic models helped explain the main mechanisms and specific kinetic features of each system. For many metal–resin combinations, the PSO model showed a strong fit to the experimental data, with determination coefficients (R^2) ranging from 98% to 100%.

Table 1. Summary of the kinetic model fitting results for various metal–resin pairs. For each combination, the best-fitting kinetic model (PSO or PFO) is indicated, along with the corresponding correlation coefficients R^2 for the PFO and PSO models, and kinetic constants $K1$ for PFO (in min^{-1}) and $K2$ for PSO (in $\text{g}/(\text{mg}\cdot\text{min})$). The table highlights the adsorption behavior and model accuracy for each metal–resin pair, showing which kinetic model best describes the ion exchange process. Blank entries indicate cases where data were not available or where the model did not adequately describe the adsorption process.

| Metal–Resin | Best Model | R^2 (%) (PFO) | R^2 (%) (PSO) | $K1$ (min^{-1}) | $K2$ ($\text{g}/\text{mg}\cdot\text{min}$) |
|--------------------------|------------|-----------------|-----------------|----------------------------|--|
| Cu^{2+} —PS—DVB | PSO | --- | 99.9 | --- | 0.002 |
| Cu^{2+} —PA—DVB | PSO | --- | 98.6 | --- | 0.00033 |
| Cu^{2+} —TFSA | PFO | 98.0 | --- | 0.0704 | --- |
| Cu^{2+} —OGL | --- | --- | --- | --- | --- |
| Pb^{2+} —PS—DVB | PSO | --- | 99.5 | --- | 0.00021 |
| Pb^{2+} —PA—DVB | PFO | 98.3 | --- | 0.0377 | --- |
| Pb^{2+} —TFSA | PSO | --- | 99.5 | --- | 0.0008 |
| Pb^{2+} —OGL | --- | --- | --- | --- | --- |
| Co^{2+} —PS—DVB | PSO | --- | 99.7 | --- | 0.000576 |
| Co^{2+} —PA—DVB | PFO | 97.8 | --- | 0.127 | --- |
| Co^{2+} —TFSA | PSO | --- | 99.8 | --- | 0.0605 |
| Co^{2+} —OGL | --- | --- | --- | --- | --- |
| Ni^{2+} —PS—DVB | PSO | --- | 98.3 | --- | 0.00079 |
| Ni^{2+} —PA—DVB | PFO | 97.8 | --- | 0.126 | --- |
| Ni^{2+} —TFSA | --- | --- | --- | --- | --- |
| Ni^{2+} —OGL | --- | --- | --- | --- | --- |

The PS—DVB resin proved to be very versatile and particularly efficient in the adsorption of various metal cations, predominantly following the second-order kinetic model (PSO). This suggests that the adsorption process involves specific chemical interactions between the active sites of the resin and the metal ions. For Cu^{2+} , it showed a PSO R^2 -value of 99.9%, suggesting very good fit and chemical adsorption, despite K_2 being relatively low (0.002 g/(mg*min)). This suggests moderate kinetics for copper on PS—DVB. For Pb^{2+} , PS—DVB fit the PSO model well ($R^2 = 99.5\%$), but the K_2 was relatively low (0.00021 g/(mg*min)), indicating slow adsorption kinetics for this metal. For Co^{2+} , the PS—DVB resin showed a good fit to the PSO model ($R^2 = 99.7\%$), with a K_2 constant of 0.000576 g/(mg*min), indicating moderate adsorption kinetics. Finally, for nickel (Ni^{2+}), the PSO model also fit well ($R^2 = 98.3\%$), although the K_2 constant was lower (0.00079 g/(mg*min)), indicating a slow adsorption rate. We can, therefore, conclude that PS—DVB proved to be an effective resin for the removal of the tested metals.

The PA—DVB resin exhibited a different behavior, fitting both the second-order (PSO) and first-order (PFO) models depending on the target metal, suggesting the possibility of mixed adsorption mechanisms. For Cu^{2+} , PA—DVB fit the PSO model better ($R^2 = 98.6\%$), with a K_2 constant of 0.00033 g/(mg*min), indicating slower adsorption kinetics than the PS—DVB resin for this metal. For Pb^{2+} , PA—DVB showed a better fit with the first-order (PFO) model, with an R^2 value of 98.3% and a K_1 constant of 0.0377 min^{-1} . In the case of cobalt (Co^{2+}), PA—DVB showed a good fit to the PFO model, with an R^2 value of 97.8% and a K_1 constant of 0.127 min^{-1} . For Ni^{2+} , the PFO model was the best ($R^2 = 97.88\%$), with a K_1 constant of 0.126 min^{-1} . In conclusion, the trends obtained using the PA—DVB resin seem to be better explained by the PFO model for some metals, such as Pb^{2+} , Co^{2+} , and Ni^{2+} , while for Cu^{2+} , it seemed to be better explained using the PSO model.

With the use of the TFSA resin, Cu fit better to the PFO model, with an R^2 value of 98% and a rate constant K_1 of 0.07047 min^{-1} , suggesting faster adsorption. For Pb^{2+} , the PSO model fit well ($R^2 = 99.5$), with a rate constant K_2 of 0.0008 g/(mg*min), suggesting moderate adsorption kinetics.

Finally, the OGL resin showed limited data for most metals, indicating poor affinity or limited adsorption capacity. The lack of data may suggest that OGL is unable to significantly adsorb metals or that its structure is not particularly suitable for these applications. This makes this particular OGL less versatile compared to the other resins tested, and potentially useful only for highly specific or selective applications. However, further physical–chemical modification of lignin may alter its properties to strengthen the adsorption of metal ions. For certain metal–resin pairs, it was not possible to calculate the statistical parameters (R^2) and kinetic constants (K_1 and K_2). This occurs when the experimental data do not follow the trends predicted by either the pseudo-first-order (PFO) or pseudo-second-order (PSO) kinetic models. When this happens, it can be inferred that no significant chemical–physical interactions develop between the resin and the specific metal, making the adsorption process inefficient.

In other cases, such as the Ni^{2+} –OGL pair, where the graph shows a clear reduction in Ni concentration, the experimental data did not fit well with either of the selected kinetic models. Careful observation shows that for both the OGL and TFSA resins, the adsorption and desorption phenomena occurred within the observed time range, which may complicate the application of kinetic models that better describe this type of process. Further investigations will be conducted to explore this behavior.

However, some researchers argue that the pseudo-first-order (PFO) model is particularly suited for describing the initial phases of adsorption kinetics but fails to adequately represent the entire process, which is more comprehensively described by the pseudo-second-order model [33]. Nevertheless, this interpretation does not explain the superior fit of one model over another, and these empirical models cannot provide mechanistic insights into the adsorption phenomena. Adsorption kinetics are governed by multiple concurrent mechanisms, encompassing both diffusive and chemical processes, and the

pseudo-first and pseudo-second-order models alone are insufficient to identify all the involved mechanisms [34,35].

While empirical kinetic models are widely employed to describe resin adsorption processes, it is crucial to acknowledge their interpretative limitations. A comprehensive understanding of the adsorption process necessitates an integrated approach that considers both mass transport phenomena (external diffusion, intraparticle diffusion) and specific chemical interactions between the adsorbate and adsorbent. Only through this broader perspective can an accurate description of the governing mechanisms be achieved, thereby enabling optimization of the system’s operational parameters.

3.3. Cation Exchange Capacity

The experimental and theoretical adsorption results for the different metal-resin combinations are reported in Table 2, which compares the experimental value of equilibrium adsorption capacity (*qe exp.*), the calculated value (*qe calc.*), the associated percentage error, and the metal removal percentage from the solution. The PS—DVB resin showed excellent removal capacities for all the tested metals, with *qe exp.* values very close to those predicted by kinetic models, as indicated by the low percentage errors. In the case of Cu²⁺, it achieved a *qe exp.* of 184.85 mg/g with an error of 6.07% and a removal rate of 98.8%, demonstrating particular effectiveness. The performance was also remarkable for Pb²⁺, with a capacity of 1994.8 mg/g, a minimal error of 0.26%, and a removal rate of 96.49%. For Ni²⁺, PS—DVB maintained a good result, showing very low *qe* errors (5.99%) and a removal percentage equal to 66.02%. Only for Co²⁺ did the removal rate reduce to 51.18%, though still maintained a low *qe* error of 1.93%. Overall, this resin demonstrated exceptional removal capacity for almost all the tested metals.

Table 2. Experimental and theoretical adsorption results for metal–resin pairs. For each metal (Cu²⁺, Pb²⁺, Co²⁺, Ni²⁺) and resin (PS—DVB, PA—DVB, TFSA, OGL), the table shows the calculated *qe calc.* value (equilibrium adsorption capacity in mg/g), the experimental *qe exp.* value, the percentage error of *qe* (*error qe*), and the metal removal percentage from the solution. Blank entries indicate the absence of available data or low affinity of the resin for the specific metal. The table allows for a comparison of adsorption efficiency and the accuracy of kinetic models for each metal–resin combination.

| Metal–Resin | <i>qe calc.</i> (mg/g) | <i>qe exp.</i> (mg/g) | Error <i>qe</i> (%) | Removal (%) |
|--------------------------|------------------------|-----------------------|---------------------|-------------|
| Cu ⁺⁺ —PS—DVB | 196.07 | 184.85 | 6.07 | 98.8 |
| Cu ⁺⁺ —PA—DVB | 158.73 | 109.64 | 44.78 | 61.32 |
| Cu ⁺⁺ —TFSA | 74.11 | 68.78 | 7.75 | 36.47 |
| Cu ⁺⁺ —OGL | --- | --- | --- | 7.05 |
| Pb ⁺⁺ —PS—DVB | 2000 | 1994.8 | 0.26 | 96.49 |
| Pb ⁺⁺ —PA—DVB | 1595.5 | 1642.31 | 2.85 | 79.44 |
| Pb ⁺⁺ —TFSA | 833.33 | 797.31 | 4.52 | 38.57 |
| Pb ⁺⁺ —OGL | --- | --- | --- | 6.16 |
| Co ⁺⁺ —PS—DVB | 833.33 | 817.57 | 1.93 | 51.18 |
| Co ⁺⁺ —PA—DVB | 704.04 | 485.07 | 45.14 | 30.36 |
| Co ⁺⁺ —TFSA | 181.82 | 179.41 | 1.34 | 10.78 |
| Co ⁺⁺ —OGL | --- | --- | --- | --- |
| Ni ⁺⁺ —PS—DVB | 434.78 | 462.48 | 5.99 | 66.02 |
| Ni ⁺⁺ —PA—DVB | 704.04 | 598.48 | 17.64 | 85.44 |
| Ni ⁺⁺ —TFSA | --- | --- | --- | 84.86 |
| Ni ⁺⁺ —OGL | --- | --- | --- | 78.58 |

The PA—DVB resin showed varying performance depending on the metal ion in solution. For Cu²⁺, the *qe exp.* (109.64 mg/g) was lower than that of PS—DVB, with a relatively high error of 44.78% and a removal rate of 61.32%. For Pb²⁺, it obtained a *qe exp.* of 1642.31 mg/g, an error of 2.85%, and a removal rate of 79.44%, showing good efficiency,

though lower than PS—DVB. For Co^{2+} and Ni^{2+} , the removal rates were 30.36% and 85.44%, respectively, suggesting variable selectivity for different metals.

The TFSA resin generally showed lower removal capacities compared to the previous resins for almost all the tested metal ions. For Cu^{2+} , it reached a $q_e \text{ exp}$ of 68.78 mg/g, an error of 7.75%, and a removal rate of 36.47%, indicating low affinity. Pb^{2+} removal was also reduced, with a $q_e \text{ exp}$ of 797.31 mg/g, an error of 4.52%, and a removal rate of 38.57%. For Co^{2+} , it showed a low $q_e \text{ exp}$ of 179.41 mg/g, an error of 1.34%, and a removal rate of 10.78%. The lack of data for Ni^{2+} further limited the overall assessment.

Data for the OGL resin were not available for any of the considered metals, making it impossible to perform a comparative analysis of its performance relative to the other resins under the tested conditions.

The examination of our experimental results indicates that the PS—DVB and PA—DVB resins exhibited (expectedly) high ion exchange capacities against the tested metals, with PS—DVB showing superiority in this panel, both in terms of removal effectiveness and accuracy of the inferred kinetic models. On the other hand, the TFSA resin boasted a mix of interesting performances and significant limitations in applications requiring efficient ion exchange. Lastly, OGL performed well vs. Ni^{2+} , which represents a novel observation and cannot be compared to any prior experimental data in the literature. The inferiority of the novel materials (i.e., TFSA-Nafion and OGL-lignin) did not come as a surprise in a comparison against highly optimized materials. Even though the PS—DVB resin provided an excellent short-term option in demanding water applications, such as the mining industry, our results also clearly demonstrated the ion exchange properties of TFSA-Nafion and OGL-lignin, which can be further engineered to formulate more sustainable next-generation resins that can bridge the gap with the current filtering technology in terms of performance and recyclability.

Nafion is an ionomeric polymer widely used in various industrial fields and recently investigated for applications in water treatment. In the literature, Nafion is primarily employed in the energy sector, specifically in fuel cells and hydrogen electrolyzer production, thanks to its exceptional proton conduction properties. However, alternative applications are emerging, including the sequestration of metal cations from aqueous solutions.

Nasel et al. [24] conducted a study on the recovery of the same metal cations studied by us using Nafion™ 117, demonstrating the material's effective behaviour in capturing such species. The results highlight that most of the sequestration occurs in the first few minutes of exposure, with a plateau reached within 30 min; specifically, the most significant absorption was recorded within the first 15 min. Similarly, in our experiments, we observed that the primary absorption occurred even more rapidly, in some cases within 5 min, with complete saturation reached around 30 min. Nasel's study also showed a strong affinity of Nafion for various metal cations, with a particular preference for Ni^{2+} , a result also confirmed in our experiments. Another relevant aspect is that the experimentation conducted at room temperature produced results comparable to those obtained by Nasel in a temperature range between 25 °C and 65 °C, confirming that temperature does not significantly influence sequestration performance.

A further promising application area for Nafion is the recovery of heavy metals from water through electrodialysis, using the material in membrane form rather than resin, in the presence of an electric field. The work by Tzanetakis et al. [36] demonstrated how Nafion, integrated into an electrodialysis system, allows for the separation and recovery of Ni^{2+} and Co^{2+} ions from sulphate-containing solutions. In this context, the focus was not on permanent ion sequestration, but on their temporary capture and subsequent efficient transfer through the membrane during the electrodialysis process. This study highlights Nafion's high affinity for the analyzed metals, further supporting the idea that it could be a highly promising material for the separation and treatment of ionic species.

Unlike Nafion, lignin offers a significantly broader range of applications. However, compared to our study, in which we used untreated lignin to evaluate its absorption performance in its natural form, the scientific literature shows a preference for the chemical

treatment of lignin. These treatments allow for the introduction of new functional groups and improve the accessibility of existing ones, thus enhancing its adsorbent properties.

For example, in the work by Xu et al. [37], amine groups were introduced through the Mannich reaction, resulting in a significant improvement in copper ion chelation and adsorption capacity. For lead ions, Li et al. [38] added -CSS groups, increasing the complexation capacity with this metal. Another example is the work by Zhang et al. [39], which produced a doubly modified lignin with -CSS and -COOH groups, creating a highly effective material for lead adsorption. In Wysokowski et al. [40], Kraft lignin was combined with chitin, after modification with a 15% hydrogen peroxide solution. This combination produced a material enriched with available functional sites, such as phenolic OH and -COOH groups, thus increasing the number of active sites on the surface.

Regarding cobalt sequestration, Budnyak et al. [41] used Kraft lignin subjected to aminomethylation for the introduction of amine groups, useful for subsequent interactions with silica. This composite material demonstrated the coordination and adsorption capacity of cobalt ions in aqueous solution three times higher than the starting materials.

In conclusion, the results obtained from this study demonstrate the effectiveness of various cation exchange resins in treating contaminated water and recovering critical materials. Traditional resins such as PS—DVB and PA—DVB, with their high capacity for removing heavy metals, are particularly well-suited for established industrial applications, such as the treatment of industrial and mining wastewater. These resins provide an immediately implementable option in existing treatment systems, enhancing efficiency and ensuring compliance with environmental regulations. The innovative material TFSA, based on recycled Nafion, has shown good removal capabilities for metals such as Cu, Pb, Ni²⁺, and Ag⁺, although with a generally lower performance compared to commercial resins. Nevertheless, TFSA represents a sustainable and technologically advanced alternative, particularly interesting for the selective recovery of critical metals and for applications where sustainability is a key factor. OGL, derived from lignin, offers an ecological and renewable solution, with particular effectiveness for nickel, although it requires further optimization to achieve performance comparable to traditional resins. It is important to emphasize, however, that any chemical modification of lignin to enhance its properties, such as the introduction of -CSS functional groups through the use of carbon disulfide (CS₂), must be approached with utmost responsibility. CS₂ is highly toxic, and its use poses a significant risk to human health and the environment. For this reason, the development of lignin-based materials must adopt an approach that balances innovation and sustainability, promoting eco-friendly and low-impact processes. These innovative materials pave the way for the next generation of ion exchange resins, combining high performance, environmental sustainability, and targeted applications. As such, the recovery of Critical Raw Materials (CRMs) from industrial wastewater would not only reduce dependence on primary sources, but would also contribute to mitigating the risks associated with global supply chains, while promoting more sustainable water treatment technologies.

4. Conclusions

In this study, we evaluated the metal adsorption efficiency of four cation exchange resins (PS—DVB, PA—DVB, TFSA, and OGL) from single-metal aqueous solutions, with a particular focus on Critical Raw Materials (CRMs) such as Cu²⁺, Co²⁺, Ni²⁺, Ag⁺, and Pb²⁺. The investigation focused on removal kinetics and adsorption performance parameters.

The results demonstrated that PS-DVB showed superior removal efficiency across all metals, with pseudo-second-order adsorption kinetics. PA-DVB's efficiency was more variable, achieving 85.44% removal for Ni²⁺ in particular. The TFSA resin displayed an overall lower adsorption capacity but demonstrated specific selectivity for certain metals, especially Ni²⁺ (84.86% removal). The lignin-derived OGL resin, despite showing limited overall removal capacity under experimental conditions, exhibited notable selectivity for Ni²⁺, with a removal efficiency of 78.58%. This suggests potential applications in sustainable and selective Ni²⁺ recovery processes, although further optimization studies

are warranted to enhance its broader applicability. Therefore, while conventional resins (PS—DVB and PA—DVB) remain highly effective for broad-spectrum metal removal in current industry, innovative materials like TFSA show potential for selective metal recovery applications, especially if further developed and engineered for specific applications. This selectivity could be particularly valuable for targeted CRM recovery in industrial processes. The results of this work are relevant to both water treatment and Critical Raw Material recovery. The proposed approach may provide valuable guidance for selecting appropriate materials for specific metal removal applications, contributing to both environmental protection and resource recovery objectives. Future research should focus on (i) investigating the performance of these ion exchange materials under competitive multi-metal conditions, (ii) developing enhanced Nafion-based and lignin-based matrix materials, and (iii) optimizing operational parameters for selective metal recovery. Additionally, studies on resin material regeneration, life cycle, and economic viability assessment for large-scale applications will be crucial for industrial implementation.

Supplementary Materials: The following supporting information can be downloaded at: <https://www.mdpi.com/article/10.3390/separations11120357/s1>, Figure S1: Time-dependent concentration of available Ag⁺ metal ions in bulk solution (ppm) examined by ICP-EOS; Table S1: Summary of kinetic model fitting results for various Ag⁺-resin pairs; Table S2: Experimental and theoretical adsorption results for Ag⁺-resin pairs. Figure S2: Morphological characterization of ion exchange resins: PS—DVB (A), PA—DVB (B), TFSA (C), and OGL (D).

Author Contributions: Conceptualization, L.A.H., S.B., A.P. and A.R.; methodology, L.A.H., S.B., and A.P.; validation, L.A.H., S.B., G.M., R.H. and A.R.; formal analysis, L.A.H., S.B. and L.S.; investigation, S.B., L.S. and L.A.H.; resources, R.H., G.M. and A.P.; data curation, S.B.; writing—original draft preparation, S.B.; writing—review and editing, all authors; supervision, A.P. and A.R.; project administration, L.A.H. and A.R.; funding acquisition, L.A.H. and A.R. All authors have read and agreed to the published version of the manuscript.

Funding: L.A.H. and S.B. acknowledge that this research was partially funded by the European Commission through the I4-GREEN Project, grant number 101084028. APC has been kindly waived by MDPI.

Data Availability Statement: Data are contained within the article or Supplementary Material.

Conflicts of Interest: The authors Luis Alexander Hein and Sara Bergamasco were employed by the company Nanofaber S.r.l. These authors declare that Nanofaber S.r.l. contributed to the methodology and the manufacturing of the prototype materials on its premises in the scope of the referenced EU project I4GREEN. Antonio Rinaldi is also affiliated with Nanofaber S.r.l. as a co-founder. The author Giampiero Menegatti was employed by the company Poirino SpA, which took part in the experiments. The remaining authors declare no other disclosures and that the research was conducted in the absence of any commercial or financial relationships that could be construed as potential conflicts of interest. The funders had no role in the design of the study; in the collection, analyses, or interpretation of data; in the writing of the manuscript; or in the decision to publish the results. All authors took the decision to submit the manuscript and conducted the research in the absence of any commercial or financial relationships that could be construed as potential conflicts of interest. In particular, this work does not represent work for hire, paid advertisement, or work for profit because it was supported by public funding from H2020 projects by the EC.

References

1. Van Gaalen, J.M.; Chris Slootweg, J. From Critical Raw Materials to Circular Raw Materials. *ChemSusChem* **2024**, e202401170. [[CrossRef](#)] [[PubMed](#)]
2. Rabe, W.; Kostka, G.; Stegen, K.S. China's supply of critical raw materials: Risks for Europe's solar and wind industries? *Energy Policy* **2017**, *101*, 692–699. [[CrossRef](#)]
3. Malpede, M. The Dark Side of Batteries: Education, Fertility and Cobalt Mining in the Democratic Republic of Congo; Working Paper Series. 2020. Available online: https://papers.ssrn.com/sol3/papers.cfm?abstract_id=3680730 (accessed on 17 September 2020).
4. Hynek, O. China's Rare Earth Monopoly: Implications for Western Security. *Cent. Eur. J. Politics* **2023**, *9*, 13–32. [[CrossRef](#)]

5. Nakhjiri, A.T.; Sanaeepur, H.; Amooghin, A.E.; Shirazi, M.M.A. Recovery of precious metals from industrial wastewater towards resource recovery and environmental sustainability: A critical review. *Desalination* **2022**, *527*, 115510. [[CrossRef](#)]
6. Dobson, R.S.; Burgess, J.E. Biological treatment of precious metal refinery wastewater: A review. *Miner. Eng.* **2007**, *20*, 519–532. [[CrossRef](#)]
7. Karvelas, M.; Katsoyiannis, A.; Samara, C. Occurrence and fate of heavy metals in the wastewater treatment process. *Chemosphere* **2003**, *53*, 1201–1210. [[CrossRef](#)] [[PubMed](#)]
8. Bilal, M.; Shah, J.A.; Ashfaq, T.; Gardazi, S.M.H.; Tahir, A.A.; Pervez, A.; Haroon, H.; Mahmood, Q. Waste biomass adsorbents for copper removal from industrial wastewater—A review. *J. Hazard. Mater.* **2013**, *263*, 322–333. [[CrossRef](#)] [[PubMed](#)]
9. Kyzas, G.Z.; Matis, K.A. Flotation in water and wastewater treatment. *Processes* **2018**, *6*, 116. [[CrossRef](#)]
10. Saleh, T.A.; Mustaqeem, M.; Khaled, M. Water treatment technologies in removing heavy metal ions from wastewater: A review. *Environ. Nanotechnol. Monit. Manag.* **2022**, *17*, 100617. [[CrossRef](#)]
11. Alexandratos, S.D. Ion-exchange resins: A retrospective from industrial and engineering chemistry research. *Ind. Eng. Chem. Res.* **2009**, *48*, 388–398. [[CrossRef](#)]
12. Barman, M.K.; Bhattarai, A.; Saha, B. Applications of ion exchange resins in environmental remediation. *Vietnam J. Chem.* **2023**, *61*, 533–550. [[CrossRef](#)]
13. Jasim, A.Q.; Ajjam, S.K. Removal of heavy metal ions from wastewater using ion exchange resin in a batch process with kinetic isotherm. *S. Afr. J. Chem. Eng.* **2024**, *49*, 43–54. [[CrossRef](#)]
14. Wu, W.; Miao, F.; Shang, R.; Liu, Y.; Liu, Y.; Jiao, W. A method for the efficient removal of Pb (II) by D001 resin in a rotating packed bed. *Chem. Eng. Process.-Process Intensif.* **2024**, *196*, 109635. [[CrossRef](#)]
15. Bensalah, J.; Ouaddari, H.; Erdoğan, Ş.; Tüzün, B.; Gaafar, A.-R.Z.; Nafidi, H.-A.; Bourhia, M.; Habsaoui, A. Cationic resin polymer A[®] IRC-50 as an effective adsorbent for the removal of Cr (III), Cu (II), and Ag (I) from aqueous solutions: A kinetic, mathematical, thermodynamic and modeling study. *Inorg. Chem. Commun.* **2023**, *157*, 111272. [[CrossRef](#)]
16. Dizge, N.; Keskinler, B.; Barlas, H. Sorption of Ni (II) ions from aqueous solution by Lewatit cation-exchange resin. *J. Hazard. Mater.* **2009**, *167*, 915–926. [[CrossRef](#)]
17. Msumange, D.A.; Yazici, E.Y.; Celep, O.; Devci, H.; Kritskii, A.; Karimov, K. Recovery of Au and Ag from the roasted calcine of a copper-rich pyritic refractory gold ore using ion exchange resins. *Miner. Eng.* **2023**, *195*, 108017. [[CrossRef](#)]
18. Pehlivan, E.; Altun, T. The study of various parameters affecting the ion exchange of Cu²⁺, Zn²⁺, Ni²⁺, Cd²⁺, and Pb²⁺ from aqueous solution on Dowex 50W synthetic resin. *J. Hazard. Mater.* **2006**, *134*, 149–156. [[CrossRef](#)]
19. Sgreccia, E.; Rogalska, C.; Gallardo Gonzalez, F.S.; Proposito, P.; Burratti, L.; Knauth, P.; Di Vona, M.L. Heavy metal decontamination by ion exchange polymers for water purification: Counterintuitive cation removal by an anion exchange polymer. *J. Mater. Sci.* **2024**, *59*, 2776–2787. [[CrossRef](#)]
20. Skvortsova, L.; Tyo, A.; Zakharova, E.; Shelkovnikov, V. Isolation of Mn (II), Fe (III), Cu (II) and Ni (II) ions on strongly acidic cation-exchange resins followed by determination of inorganic arsenic by anodic stripping voltammetry. *AIP Conf. Proc.* **2016**, *1772*, 020014. [[CrossRef](#)]
21. Silva, R.; Passerini, S.; Pozio, A. Solution-cast Nafion[®]/montmorillonite composite membrane with low methanol permeability. *Electrochim. Acta* **2005**, *50*, 2639–2645. [[CrossRef](#)]
22. Chen, Z.; Patel, R.; Berry, J.; Keyes, C.; Satterfield, C.; Simmons, C.; Neeson, A.; Cao, X.; Wu, Q. Development of Screen-Printable Nafion Dispersion for Electrochemical Sensor. *Appl. Sci.* **2022**, *12*, 6533. [[CrossRef](#)]
23. Huang, F.; Jin, Y.; Wen, L.; Wan, Z. Nafion modification of thermal-oxidized IrOx electrode. *J. Electrochem. Soc.* **2018**, *165*, B12. [[CrossRef](#)]
24. Nasef, M.M.; Yahaya, A.H. Adsorption of some heavy metal ions from aqueous solutions on Nafion 117 membrane. *Desalination* **2009**, *249*, 677–681. [[CrossRef](#)]
25. Ge, Y.; Li, Z. Application of lignin and its derivatives in adsorption of heavy metal ions in water: A review. *ACS Sustain. Chem. Eng.* **2018**, *6*, 7181–7192. [[CrossRef](#)]
26. Song, Z.; Li, W.; Liu, W.; Yang, Y.; Wang, N.; Wang, H.; Gao, H. Novel magnetic lignin composite sorbent for chromium (VI) adsorption. *RSC Adv.* **2015**, *5*, 13028–13035. [[CrossRef](#)]
27. Bergrath, J.; Rumpf, J.; Burger, R.; Do, X.T.; Wirtz, M.; Schulze, M. Beyond yield optimization: The impact of organosolv process parameters on lignin structure. *Macromol. Mater. Eng.* **2023**, *308*, 2300093. [[CrossRef](#)]
28. Efimova, N.V.; Krasnopyorova, A.P.; Yuhno, G.D.; Scheglovskaya, A.A. Sorption of heavy metals by natural biopolymers. *Adsorpt. Sci. Technol.* **2017**, *35*, 595–601. [[CrossRef](#)]
29. Supanchaiyamat, N.; Jetsrisuparb, K.; Knijnenburg, J.T.; Tsang, D.C.; Hunt, A.J. Lignin materials for adsorption: Current trend, perspectives and opportunities. *Bioresour. Technol.* **2019**, *272*, 570–581. [[CrossRef](#)]
30. Meenakshi, S.; Viswanathan, N. Identification of selective ion-exchange resin for fluoride sorption. *J. Colloid Interface Sci.* **2007**, *308*, 438–450. [[CrossRef](#)] [[PubMed](#)]
31. Wang, C.; Liu, J.; Zhang, Z.; Wang, B.; Sun, H. Adsorption of Cd (II), Ni (II), and Zn (II) by tourmaline at acidic conditions: Kinetics, thermodynamics, and mechanisms. *Ind. Eng. Chem. Res.* **2012**, *51*, 4397–4406. [[CrossRef](#)]
32. Mashio, T.; Malek, K.; Eikerling, M.; Ohma, A.; Kanesaka, H.; Shinohara, K. Molecular dynamics study of ionomer and water adsorption at carbon support materials. *J. Phys. Chem. C* **2010**, *114*, 13739–13745. [[CrossRef](#)]

33. Wang, C.; Wang, B.; Liu, J.; Yu, L.; Sun, H.; Wu, J. Adsorption of Cd (II) from acidic aqueous solutions by tourmaline as a novel material. *Chin. Sci. Bull.* **2012**, *57*, 3218–3225. [[CrossRef](#)]
34. Chen, H.; Wang, A. Adsorption characteristics of Cu (II) from aqueous solution onto poly (acrylamide)/attapulgite composite. *J. Hazard. Mater.* **2009**, *165*, 223–231. [[CrossRef](#)] [[PubMed](#)]
35. Tran, H.N. Is it possible to draw conclusions (adsorption is chemisorption) based on fitting between kinetic models (pseudo-second-order or elovich) and experimental data of time-dependent adsorption in solid-liquid phases? *Recent Innov. Chem. Eng. (Former. Recent Pat. Chem. Eng.)* **2022**, *15*, 228–230. [[CrossRef](#)]
36. Tzanetakis, N.; Taama, W.; Scott, K.; Jachuck, R.; Slade, R.; Varcoe, J. Comparative performance of ion exchange membranes for electrodialysis of nickel and cobalt. *Sep. Purif. Technol.* **2003**, *30*, 113–127. [[CrossRef](#)]
37. Xu, J.; Zhu, S.; Liu, P.; Gao, W.; Li, J.; Mo, L. Adsorption of Cu (ii) ions in aqueous solution by aminated lignin from enzymatic hydrolysis residues. *RSC Adv.* **2017**, *7*, 44751–44758. [[CrossRef](#)]
38. Li, Z.; Kong, Y.; Ge, Y. Synthesis of porous lignin xanthate resin for Pb²⁺ removal from aqueous solution. *Chem. Eng. J.* **2015**, *270*, 229–234. [[CrossRef](#)]
39. Zhang, Z.; Wu, C.; Ding, Q.; Yu, D.; Li, R. Novel dual modified alkali lignin based adsorbent for the removal of Pb²⁺ in water. *Ind. Crops Prod.* **2021**, *173*, 114100. [[CrossRef](#)]
40. Wysokowski, M.; Klapiszewski, Ł.; Moszyński, D.; Bartczak, P.; Szatkowski, T.; Majchrzak, I.; Siwińska-Stefańska, K.; Bazhenov, V.V.; Jesionowski, T. Modification of chitin with kraft lignin and development of new biosorbents for removal of cadmium (II) and nickel (II) ions. *Mar. Drugs* **2014**, *12*, 2245–2268. [[CrossRef](#)]
41. Budnyak, T.M.; Piątek, J.d.; Pylypchuk, I.V.; Klimpel, M.; Sevastyanova, O.; Lindström, M.E.; Gun'ko, V.M.; Slabon, A. Membrane-filtered kraft lignin–silica hybrids as bio-based sorbents for cobalt (II) ion recycling. *ACS Omega* **2020**, *5*, 10847–10856. [[CrossRef](#)] [[PubMed](#)]

Disclaimer/Publisher's Note: The statements, opinions and data contained in all publications are solely those of the individual author(s) and contributor(s) and not of MDPI and/or the editor(s). MDPI and/or the editor(s) disclaim responsibility for any injury to people or property resulting from any ideas, methods, instructions or products referred to in the content.